An Ultrasonic Motor Driven by Traveling Cylindrical Wedge Waves

Ching-Chung Yin and Tai-Ho Yu
Department of Mechanical Engineering
National Chiao Tung University
Hsinchu 300, Taiwan, R.O.C.
E-mail: ccyin@faculty.nctu.edu.tw

***Abstract*—A novel ultrasonic motor driven by flexural waves traveling circumferentially along a circular cylindrical wedge-like acoustic waveguide is presented. A rotary motion can be induced via friction forces if a rotor normally contacts the internal inclined surface of the cylindrical wedge near the tips. The rotary motor stator has a simple structure constructed by a metal cylindrical wedge adhered on a piezoelectric tube whose polarization is in the radial direction. The wedge acoustic waves are excited by two sets of comb electrodes painted on the outer surface of the piezoelectric tube. Both comb transducers with an angular space apart are excited by AC signal in $\pm 90^{o}$ phase difference to achieve bidirectional operation for the motor. There exist a number of axial modes and circumferential modes in the stator in a broad frequency range below 100 kHz. Only the fundamental modes of the latter are considered to drive this rotary motor. Along with commercial codes of finite element method (FEM), a bi-dimensional FEM has been developed to determine the resonance frequencies of circumferential modes and their corresponding modal displacements. The angular speed and direction are controllable by altering the driving voltage and the phase difference between two comb transducers.**

Keywords-Wedge wave; ultrasonic motor; circumferential mode; dual phase

I. INTRODUCTION

Acoustic wedge waves have been received lots of attentions since the first discovery by Lagasse [1] in 1972. The wedge waves are flexural waves traveling along the wedge tip. It is found that elastic energy carried by the wedge waves is confined within the area of about one wavelength near the wedge tips. Most researches focused attention on the dispersion phenomena of the flexural wave propagation along the wedge-tip using either numerical investigations or experimental observations [2-4]. The application of wedge-like acoustic waveguides in actuators was first proposed by Krylov [3] for propulsion of a small submarine. It has never become real yet.

Ultrasonic motors feature high torques at low speed, no electromagnetic interference, quick response, simple structure configuration and excellent controllability. A variety of ultrasonic motors actuated by piezoelectric ceramics were developed in the last three decades, including circular discs, annular rings, hollow tubes, and so on [5-9]. Using acoustic waveguides as motor stators is a trend of developing new ultrasonic motor. For example, the ridge-waves traveling along a ridge on a substrate were used to drive a linear ultrasonic motor by Tominaga et al. [8]. Acoustic guided waves are capable to propagate far away without energy dissipation since particles resonantly oscillate in each cross section of the elastic waveguides.

This paper presents a new rotary traveling wave ultrasonic motor using acoustic wedge-waves. Instead of unnecessary compromise with commercial codes on loss of accuracy and poor efficiency, a bi-dimensional FEM is developed to analyze the resonant frequencies and vibration modes of the circumferential flexural waves. Several possible designs are described and discussed. In addition, a prototype of the motor has been fabricated and its performance test has also been carried out experimentally.

II. VIBRATIONAL ANALYSIS

Fig. 1 shows the proposed wedge-wave ultrasonic motor stator schematically. The motor stator is constructed by a metal cylindrical wedge adhered on a piezoelectric tube with its polarization in the radial direction. A practical stator configuration is required to have fixed ends, where the cylindrical stator is clamped at its bottom. Two sets of comb transducers with an angular space apart are located on the wall of the piezoelectric tube to induce two standing waves. A traveling wave is formed by the constructive interference of two standing waves with a temporal phase shift. Both traveling waves and standing waves are operated at near resonance frequencies of the cylindrical motor stator.

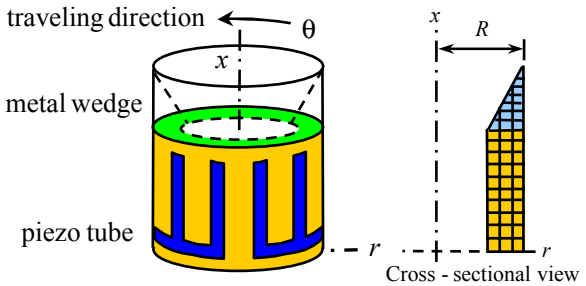

Fig.1. Schematic diagram of the proposed motor stator

The resonant vibration modes of a hollow cylinder are defined by two integers (n, m). The first integer n is the circumferential number which indicates the number of wavelengths of standing wave around the circumference. The second integer m represents that the vibration modes having m+1 axial nodes of zero displacement along the axial length of the cylinder. Modes for which $n = 1$ are the beam modes in which the cross section remains circular. Those for which $n \geq 2$ are the circumferential modes that can construct traveling flexural waves to drive the ultrasonic motors.

A. FEM Analysis

A bi-dimensional FEM [4] is adopted to determine the resonant vibration modes and phase velocities of the circumferentially flexural waves. Refer to the polar coordinate system shown in Fig. 1, whole structure of the motor stator is divided among a number of 2-dimensional discrete four-node isoparametric (Q4) elements. By separation of variables, the elastic displacements and electric displacement vector in each element is represented as

$$\begin{Bmatrix} \mathbf{u} \\ \varphi \end{Bmatrix} = \begin{Bmatrix} u_r(r,x) \\ u_x(r,x) \\ u_\theta(r,x) \\ \varphi(r,x) \end{Bmatrix} e^{j(n\theta-\omega t)} = \begin{Bmatrix} \mathbf{N}_u \mathbf{d} \\ \mathbf{N}_\phi \mathbf{\Phi} \end{Bmatrix} e^{j(n\theta-\omega t)}, \qquad (1)$$

where the circumferential number n could be a non-integer for traveling waves, but it must be an integer for standing waves. The matrices $\mathbf{N}_u$, $\mathbf{N}_\phi$ are interpolation functions in conjunction to each nodal displacements and electric displacement. It is noted that u_θ has a 90° phase lag to the other two elastic displacement components. Using Hamilton's principle, a system of equations for wedge waves traveling along the circular, cylindrical stator is derived as follows:

$$\begin{bmatrix} \mathbf{M} & 0 \\ 0 & 0 \end{bmatrix} \begin{Bmatrix} \ddot{\mathbf{d}} \\ \ddot{\mathbf{\Phi}} \end{Bmatrix} + \begin{bmatrix} \mathbf{K}_{uu} & \mathbf{K}_{u\phi} \\ \mathbf{K}_{\phi u} & \mathbf{K}_{\phi\phi} \end{bmatrix} \begin{Bmatrix} \mathbf{d} \\ \mathbf{\Phi} \end{Bmatrix} = \begin{Bmatrix} \mathbf{0} \\ 0 \end{Bmatrix}, \qquad (2)$$

where $\mathbf{M}, \mathbf{K}_{uu}, \mathbf{K}_{u\phi}, \mathbf{K}_{\phi\phi}$ are the global mass matrix and the global elastic, elasto-piezoelectric, piezoelectric stiffness matrices. If all the field variables are time-harmonic, (2) can results in a frequency equation (or dispersion equation) as follows:

$$\det\left(\begin{bmatrix} \mathbf{K}_{uu} & \mathbf{K}_{u\phi} \\ \mathbf{K}_{\phi u} & \mathbf{K}_{\phi\phi} \end{bmatrix} - \omega^2 \begin{bmatrix} \mathbf{M} & \mathbf{0} \\ \mathbf{0} & \mathbf{0} \end{bmatrix} \right) = 0 . \qquad (3)$$

The resonant modes of flexural waves can be calculated once the angular frequency $\omega = 2\pi f$ and circumferential wave number $k = n/R$ in (3) are determined.

B. Theoretical Results

As an example for numerical calculation, we consider a motor stator manufactured by a navy brass wedge adhered on a PZT-5H tube (Morgan Electro Ceramics) with polarization in the radial direction. The wedge has 15° apex angle, 9 mm height and a 40 μm truncation on the wedge tip due to machining tolerance. The PZT-5H tube is 3.5 mm thick and both its height and outer diameter are 25.4 mm. The piezoelectric tube is mounted on a navy brass base which is fixed at its bottom. A schematic diagram of the motor stator is shown in the inset of Fig. 2 with abbreviations MW, PT, and B for metal wedge, piezoelectric tube, and base.

The numerical calculations are carried out by using the bi-dimensional FEM and a commercial code (ANSYS release 10.0). Both methods require different numbers of meshes to obtain a convergent approximation. Large deformation of the wedge waves is confined within a small region near the wedge tip [1]. The wedge-tip region demands a larger number of meshes than those regions far away from the tip. In the case of motor stator shown in the inset of Fig. 2, the present method uses 2700 2-D elements (Q4) in calculation. But 47,320 3-D elements (solid-5) are used by ANSYS. The present method has an advantage that only fewer 2-D elements are required since a propagator $e^{j(n\theta-\omega t)}$ is adopted in the formulation. In addition, it does not need to increase the number of meshes for calculating various circumferential modes. A large number of elements are desirable by using ANSYS to obtain convergent approximations to higher circumferential modes.

The dispersion curves of frequency verse circumferential wave number k for the lowest five modes ($m \leq 5$) of the flexural waves are shown in Fig. 2. Basically, the flexural waves generated in circular cylindrical motor stators propagate in both clockwise and counterclockwise directions. Standing waves including beam mode and circumferential modes can be formed along the wedge tip by two-directional flexural waves of integer circumferential number (n = 1, 2, 3, etc.) and equal amplitude. The solid circles in Fig. 2 indicate those resonant frequencies of standing waves in the fundamental mode (m = 1) calculated by using ANSYS. There is an excellent agreement between the results obtained by these two methods even though deviation for which $n \geq 10$ becomes a little large. The agreement validates the bi-dimensional FEM.

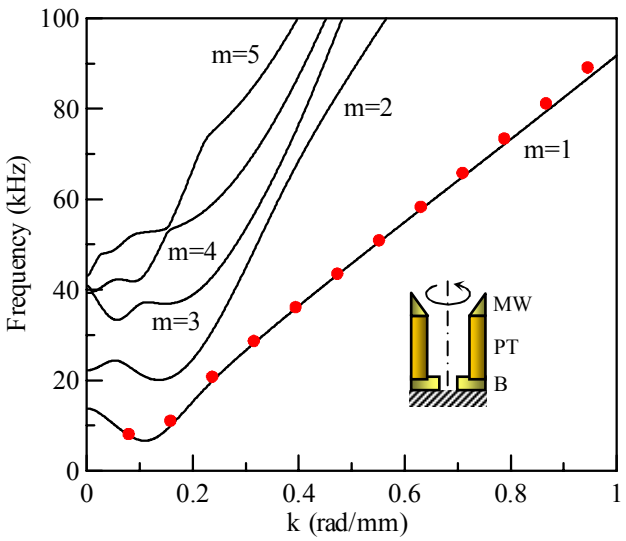

Fig. 2. Comparison of calculated dispersion curves (solid lines) for traveling flexural waves with the resonant frequencies of circumferential modes (circles) for the motor stator shown in the inset.

Complex deformation at the wedge-tip region results in a need of a tremendous number of elements by using ANSYS to determine those localized vibrations accurately. The agreement becomes poor in calculations of those higher modes ($m \geq 2$) by these two methods. Hence, the resonant frequencies of higher modes are not shown in Fig. 2 along with those dispersion curves determined by bi-dimensional FEM.

Fig. 3 depicts the amplitude of radial displacement along the outer edge of the motor stator shown in the inset of Fig. 2 for the first wedge mode (m=1). It clearly shows that the largest radial deformation occurs at the wedge tip. As the circumferential number increases, deformation is gradually confined to the wedge tip. Modes for which $n \leq 3$ have apparent displacements over the piezoelectric tube. The ideal motor stators should have very small deformation in the piezoelectric region to prevent from being disastrously burned down. Those for which $n \geq 4$ in this case are good to be motor stators.

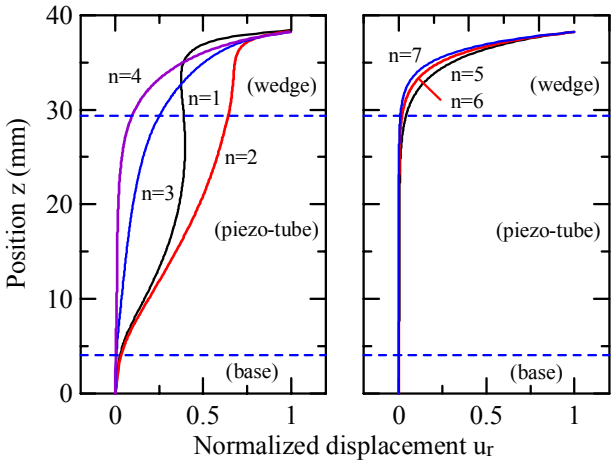

Fig. 3. The first seven circumferential modes of the motor stator 1 along its outer edge for m = 1

An ultrasonic motor utilizes mechanical vibration or traveling wave in the stator to generate sliding motion of the rotor via friction forces. An elliptical motion is desired for particles at the interface between the stator and the rotor. The ratio of circumferential displacement to radial displacement plays an important role on the elliptical motion. The greater ratio indicates that larger friction force can be induced for sliding motion. Instead of a sketch of displacement ratio along the inclined interface, the displacement ratios along the same outer edge of the stator are depicted in Fig. 4 in order to compare with the corresponding radial displacements shown in Fig. 3.

The displacement ratios at the wedge tip are close to zero. It means that the wedge tip is not able to provide enough friction force for sliding motion even though it has the largest radial displacement. The largest absolute value of displacement ratio occurs somewhere below the wedge tip. The largest ratio for which $n \geq 4$ appears at the piezoelectric tube. However, it does not mean a great friction force is induced since the radial displacement is too small to have enough circumferential displacement. The appropriate contact point between the stator and the rotor locates at the position somewhere below the wedge tip but above the piezoelectric tube.

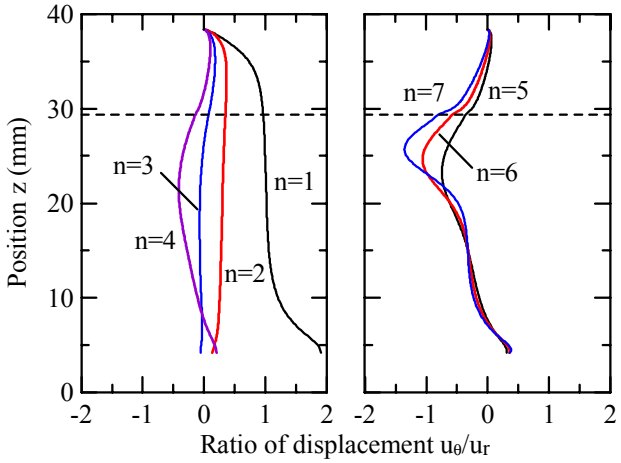

Fig. 4. Displacement ratio of u_θ / u_r in the case of Fig. 3

III. Principle of Bi-Directional Operation

Two standing wedge-waves are excited by two sets of comb electrodes painted on the outer surface of the piezoelectric tube whose inner wall is full of electrode and polarization in the radial direction. These comb transducers have stripe width equal to a quarter of wavelength. A traveling wave can be generated by the interference of two standing waves with equal amplitude and ±90° phase difference.

A bi-directional operation of the ultrasonic motor using two comb transducers in dual phase is schematically shown in Fig. 5. The angular space is defined by the interval from the left edge of one transducer to that of another. It must satisfy the following relation:

$$\theta_p = \frac{2\pi}{n}\left(p + \frac{1}{4}\right), \tag{4}$$

where p and n are integers; n indicates the circumferential number. In order to generate a traveling wave, the transducer in front of another must have a phase lag to another by $\pi/2$.

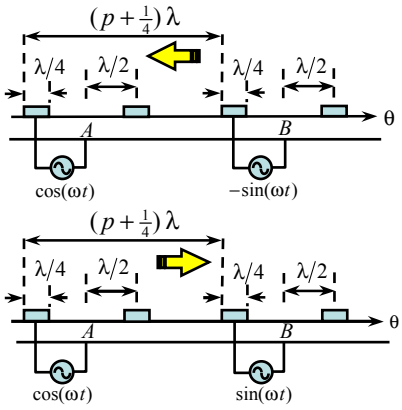

Fig. 5. Schematic of bi-directional operation by using two transducers and dual phase switching

IV. EXPERIMENTS

Fig. 6 illustrates the cross sectional diagram of two wedge-wave motor stators and the rotors for characterization. The first stator identical to the one shown in the inset of Fig.2 is used for numerical investigation. The second motor is composed of a navy brass wedge of 15° apex angle and a PZT-5A tube (Sensor Technology, Canada) which has the same dimensions as the first one except 1 mm thickness. A concave rotor of 15° inclined angle is subjected to an axial preload to contact the wedge tip of the motor stator 2.

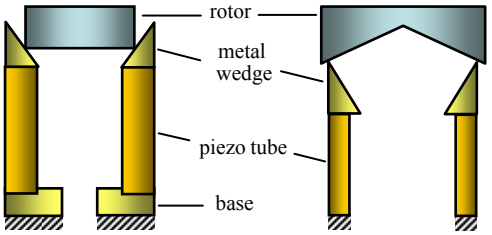

Fig. 6. Cross-sectional view of prototype motor 1 (left) and 2 (right)

The resonance frequency of the motor stator 2 has been measured by Laser Doppler Vibrometer (LDV, Sunwave Technology, Taiwan) and impedance by a HP 8751 network analyzer (Agilent Technologies, USA). Fig. 7 shows the results of resonance test. The driving frequency for excitation of mode $(n, m) = (10, 1)$ is about 68 kHz.

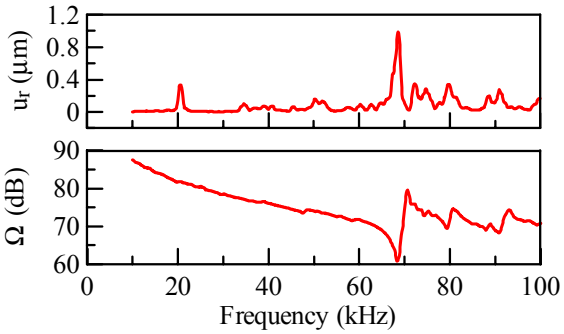

Fig. 7. Frequency response of vibration and impedance of the motor stator 2

A two-channel driving circuit composed of two power ICs PB50 (Apex Microtechnology) and several operational amplifiers is used to magnify AC signals to excite the comb transducers. The total amplifier gain is 11. The angular speed is proportional to the driving voltage. The maximum revolution speed is about 1,150 rpm. Threshold voltage of revolution is 1.2 $V_{p\text{-}p}$ in the absence of mechanical load. The results of performance tests are depicted in Fig. 8. The maximum torque output is 0.084 kg-cm.

V. CONCLUSION

An ultrasonic motor actuated by flexural waves traveling circumferentially along a circular cylindrical wedge-like compound stator has been proposed, numerically investigated, and fabricated. The performance test was carried out experimentally. In the present design, two comb transducers

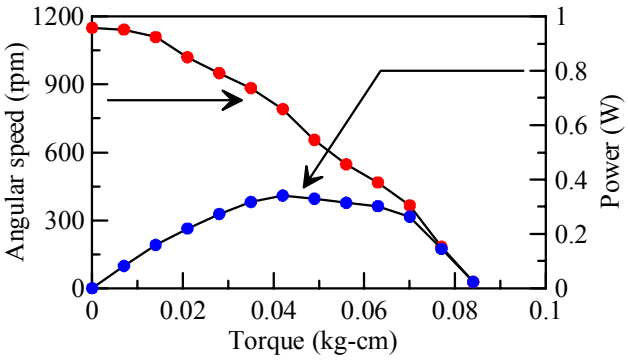

Fig. 8. Performance curves of the prototype motor 2

excited by AC signals in dual phase are used to induce a traveling wave by the interference of two standing waves with equal amplitude and 90° phase difference. A bi-directional operation for the motor is achieved by switching the phase lag between these two comb transducers.

A bi-dimensional FEM has been developed to effectively analyze resonance frequency and vibration modes of the traveling wedge-waves. According to the numerical simulation, an elliptical motion induced at the wedge tip is too small to generate enough torque for driving the rotor in spite of most deformed energy of the traveling waves confined at the region near the wedge tip. A higher output torque is expected to achieve if the contact point locates at the position that the maximum elliptical motion occurs. In the future, a further optimization will be carried out numerically by using the bi-dimensional FEM and validated experimentally.

ACKNOWLEDGMENT

This research is supported by National Science Council, Taiwan, R.O.C. under grant NSC 94-2212-E-009-003.

REFERENCES

[1] P. E. Lagasse, "Analysis of a dispersion free guide for elastic waves," *Elect. Lett.*, vol. 8, no. 15, pp. 372-373, 1972.

[2] X. Jia and M. de Billy, "Observation of the dispersion behavior of surface acoustic wave in a wedge waveguide by laser-ultrasonics," *Appl. Phys. Lett.*, vol. 61, no. 25, pp. 2970-2972, 1992.

[3] V. V. Krylov, "Propagation of wedge acoustic waves along wedges imbedded in water," *Proc. of the 1994 IEEE Ultras. Symp.*, pp. 793-796.

[4] A. C. Hladky-Hennion, "Finite analysis of the propagation of acoustic wave in waveguides," *J. Sound Vib.*, vol. 194, no. 2, pp. 119-136, 1996.

[5] T. Sashida, "A prototype ultrasonic motor - principles and experimental investigations," *Appl. Phys.*, vol. 51, pp. 17-23, 1982.

[6] N. W. Hagood and A. McFarland, "Modeling of a piezoelectric rotary ultrasonic motor," *IEEE Trans. on Ultras. Ferro. and Freq. Control*, vol. 42, no. 2, pp. 210-224, 1995.

[7] B. Koc, S. Cagatay, and K. Uchino, "A piezoelectric motor using two orthogonal bending modes of a hollow cylinder," *IEEE Trans. on Ultras. Ferro. and Freq. Control*, vol. 49, no. 4, pp. 495-500, 2002.

[8] M. Tominaga, R. Kaminaga, J. R. Friend, K. Nakamura, and S. Ueha, "An ultrasonic linear motor using ridge-mode traveling waves," *IEEE Trans. on Ultras. Ferro. and Freq. Control*, vol. 52, no. 10, pp. 1735-1742, 2005.

[9] A. Iula, and M. Pappalardo, "A high-power traveling ultrasonic motor," *IEEE Trans. on Ultras. Ferro. and Freq. Control*, vol. 53, no. 7, pp. 1344-1351, 2006.